Optical Properties of Mist CVD Grown α-Ga_2O_3

Usman Ul Muazzam, Prasad Chavan, Srinivasan Raghavan, Rangarajan Muralidharan, and Digbijoy N. Nath, *Member, IEEE*

***Abstract*— We report on the study of optical properties of mist CVD grown α-Ga_2O_3 with the observation of excitonic absorption in spectral responsivity measurements. 163 nm of Ga_2O_3 was grown on sapphire using Ga-(acac)$_3$ as the starting solution at a substrate temperature of 450°C. The film was found to be crystalline and of α-phase with an on-axis full width at half maximum (FWHM) of 92 arcsec as confirmed from X-ray diffraction scans. The Eliott-Toyozawa model was used to deduce band gap and excitonic binding energy from the absorption spectrum. The exciton binding energy was extracted to be 90 meV with large Gaussian spread of 0.195 eV. From spectral responsivity (S.R) measurements, a similar value of excitonic binding energy was found. This unusually huge binding energy is attributed to strong interaction between longitudinal optical (LO) phonons and excitons. Further, metal-semiconductor-metal (MSM) photodetectors (PD) with lateral inter-digitated geometry were fabricated on the film. A sharp band edge was observed at 229 nm (∼ 5.42 eV) in the spectral response with peak responsivity of ∼1 A/W at a bias of 20 V. The UV to visible rejection ratio was found to be ∼ 100 while the dark current was measured to be ∼ 0.1 nA at a bias voltage of 20 V.**

***Index Terms*— α-Ga_2O_3, exciton, mist CVD, MSM, UV photodetector.**

I. Introduction

THE various polymorphs of Ga_2O_3, with their wide band gap of 4.6-5.6 eV eV [1]–[3] have attracted attention of the device community for their promises in the areas of high-power switching [4], deep-UV optoelectronics [5], gas sensors [6], high-temperature and transparent electronics [7]. UV-C photodetectors for instance, are useful in UV astronomy, bio-medical and forensic applications, and for missile plume detection in the strategic sector [8]–[10]. Although the β phase is the most stable among the five different polymorphs (α, β, γ, ε, δ) of Ga_2O_3 and thus has been the most widely investigated, there has been an increasing interest in α-Ga_2O_3 in recent times. It ahas a corundum crystal structure and has been predicted to have the highest band gap (∼ 5.6 eV [11]) among all the polymorphs of Ga_2O_3. This makes α-Ga_2O_3 an attractive candidate for ultra-high breakdown transistors and deep-UV opto-electronics at sub-240 nm wavelengths. The growth of α-Ga_2O_3, which requires relatively low temperatures (430 °C – 470 °C) [12], has been reported using approaches such as mist chemical vapor deposition, atomic layer deposition (ALD) and molecular beam epitaxy [12]–[14]. Although there is a report on the demonstration of field effect transistor (FET) based on mist CVD grown α-Ga_2O_3 [15], the investigation of the growth as well as structural, optical and electrical transport properties of this emerging polymorph of Ga_2O_3 is still at an embryonic stage. In this letter, we report on the study of optical – in particular excitonic - properties of mist CVD grown α-Ga_2O_3 with a subsequent realization of a high-responsivity solar blind UV-C photodetectors.

Manuscript received February 6, 2020; revised February 14, 2020; accepted February 17, 2020. Date of publication February 27, 2020; date of current version March 12, 2020. This work was supported in part by U.S. Air Force Office of Scientific Research (AFOSR), U.S. Air Force (USAF) under Grant FA2386-19-1-4026 (Program Manager: Ali Sayir), in part by Ministry of Human Resource Development (MHRD) and Ministry of Electronics and Information Technology (MeitY) through Nanoelectronics Network For Research and Application (NNETRA), and in part by MHRD, MeitY, and the Department of Science and Technology (DST) Nano Mission for supporting the facilities at Centre for Nano Science and Engineering (CeNSE). *(Corresponding author: Usman Ul Muazzam.)*

The authors are with the Centre for Nano Science and Engineering (CeNSE), Indian Institute of Science (IISc), Bengaluru 560012, India (e-mail: usmaanm@iisc.ac.in).

Color versions of one or more of the figures in this letter are available online at http://ieeexplore.ieee.org.

Digital Object Identifier 10.1109/LPT.2020.2976450

II. Growth, Material Characterization and Fabrication

The mist CVD system used for the growths has been developed in-house and consists of two parts, the reactor and the mist generator. A volume of 0.33 mole 5N pure gallium acetylacetonate Ga(acac)$_3$ dissolved in de-ionised water (DI) was used as the gallium precursor. A small amount (0.1 ml) of HCl was added to ensure the complete dissolution of Ga(acac)$_3$ in DI water. This solution was then ultra-sonicated at a frequency of 1.6 MHz using the mist-generator. The generated mist was directed to the deposition zone using N_2 (500 sccm) as carrier gas. A c-plane sapphire wafer of 2-inch diameter was diced into 1 cm x 1 cm pieces which were solvent cleaned in acetone, isopropyl alcohol and rinsed with DI water. For each growth run, a piece of sapphire was placed inside the deposition zone using a quartz tube with diameter of 40 mm. The growth was carried out for one hour at a temperature of 450 °C and at atmospheric pressure.

The XRD scans were carried out using a Rigaku SmartLab, Cu-Ka radiation X-ray diffraction system. The film grown on sapphire was confirmed to be α-Ga_2O_3 from a θ-2θ scan. Figure 1 shows the scan of (0006) reflection of α-Ga_2O_3, and the inset to figure 1 shows the symmetric rocking curve with an FWHM of 92.2 arcsec indicative of a low screw dislocation density in the epitaxial layer. The surface morphology of the as-deposited film was studied using atomic force microscopy (Dimension ICON, Bruker) and the rms roughness was found to be 2 nm as shown in figure 2(a), which confirms the smoothness of the film. The film thickness was found to be 163 nm from ellipsometry measurements. Figure 2(b) shows the image of the as-grown film as obtained from scanning

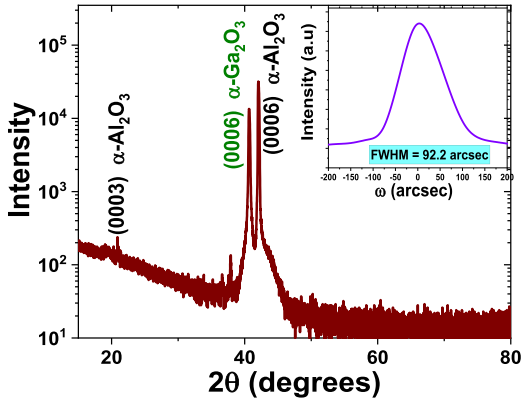

Fig. 1. XRD θ-2θ diffraction pattern of as deposited film of α-Ga_2O_3, inset shows the rocking curve of (0006) peak of α-Ga_2o_3 with FWHM of 92.2 arcsec.

electron microscopy (GEMINI Ultra 55, FE-SEM, Carl Zeiss), indicating that the layer is continuous and uniform.

Absorption spectra was measured in a UV-Vis setup (UV-3600, UV-VIS-NIR spectrophotometer, Shimadzu). The absorption spectrum (figure 3) exhibited two onsets. These features have been studied using Elliott [16] and Toyozawa [17] model developed for predicting the line-shapes of excitonic absorption. Owing to the fact that these excitonic features are visible at room temperature, expression for strong coupling limit has been invoked for fitting the experimentally observed absorption spectrum [17]. Extracted values of binding energy and direct allowed bandgap were found to be 90 meV and 5.63 eV respectively which are in close agreement with the previous reported values [3], [11]. The discrete excitonic spectrum is Gaussian like having most of the contribution from the first level only. The large Gaussian width of 0.195 eV shows interaction between excitons and phonons which will lead to an inhomogeneous broadening of absorption spectrum. This leads to the problem that higher exciton states cannot be resolved in absorption spectra but merge with the continuum if the temperature is high (because phonon population exponentially increases with temperature) [18]. The excitonic absorption dominates in the spectral region below the bandgap and for low values of the absorption coefficient it overlaps with the range of indirect transitions (which are dipole forbidden, therefore are expected to be several orders of magnitude weaker [3]). This is the cause of the small deviation of the model from the experimentally obtained absorption spectrum because the model does not account for the indirect transitions.

Photodetectors with metal-semiconductor-metal (MSM) layout in an interdigitated geometry were fabricated on the as-grown α-Ga_2O_3 sample using a standard i-line lithography process. The device schematic is shown in figure 4(a). A Ni (20 nm)/Au (100 nm) stack was deposited using sputtering to form Schottky contact. Each MSM detector as shown in figure 4(b), has seventeen pairs of interdigitated fingers where each finger has a width of 4 μm and the finger spacing is 6 μm. The active area of each device is 260 μm $\times$ 300 μm.

III. Results and Discussion

Spectral responsivity (SR) was measured using a quantum efficiency setup, the details of which are reported

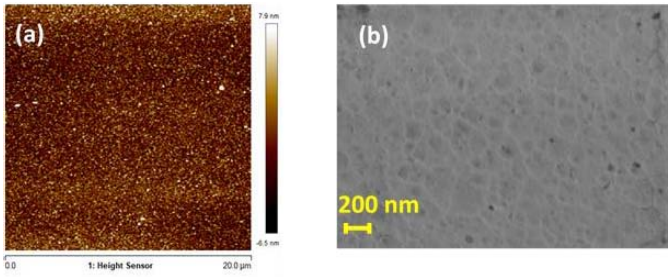

Fig. 2. (a) AFM scan image showing R.M.S roughness of 2 nm [colour scale indicates the roughness from −4.5 nm (black) to 7.9 nm (white)]. (b) SEM micrograph showing smooth morphology of as deposited film.

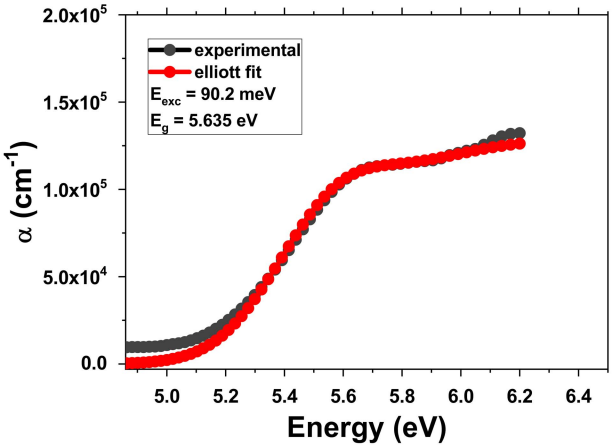

Fig. 3. Absorption edge of α-Ga_2O_3 deduced from its absorption spectrum (grey curve) and Elliott fit (red curve).

elsewhere [19]. The SR spectra exhibited a primary peak at 229 nm corresponding to band-to-band absorption while shoulder at 233 nm (5.3 eV) in Fig 5(a) in the SR spectra has been assigned to the excitonic transition. Similar feature was observed in the absorption spectra shown in Fig 3. This peak becomes less prominent at higher electric fields as expected. The other feature seen at 239 nm (5.18 eV) could be a phonon replica and it vanishes as the excitonic transition becomes weaker. It should be noted that band edge obtained from SR measurements is slightly redshifted compared to that obtained from the absorption spectrum. In contrast to the absorption measurement, spectral responsivity was measured using applied bias voltages. In the presence of an electric field, the absorption coefficient is no longer zero below the bandgap but decreases exponentially. This is because the applied electric field tilts the bands spatially and hence biasing modulates the absorption coefficient such that there is a slight red shift in the spectrum [20].

The binding energy of exciton calculated from the difference between the two peaks, was 92 meV, which is close to what we get from Elliott fit. This is also the first report of the observation of an excitonic peak in spectral response of any polymorph of gallium oxide.

To estimate the dissociation field for excitons, the effective Bohr radius of an exciton was calculated using [21]:

$$a_{\text{exc}} = a_{\text{o}} \frac{R_y}{\epsilon_s E_{exc}} \approx 8\text{Å} \quad (1)$$

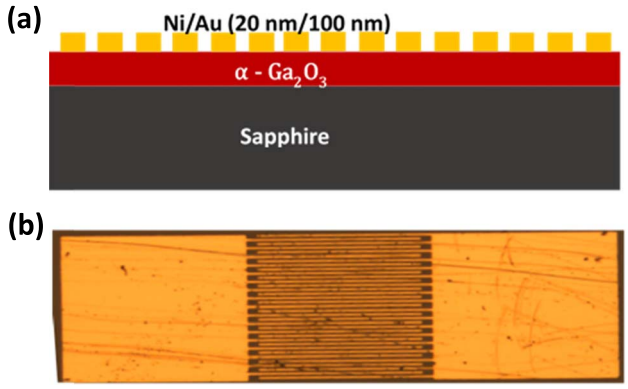

Fig. 4. (a) Schematic of MSM photodetector (side view). (b) Optical micrograph of MSM photodetector (top view).

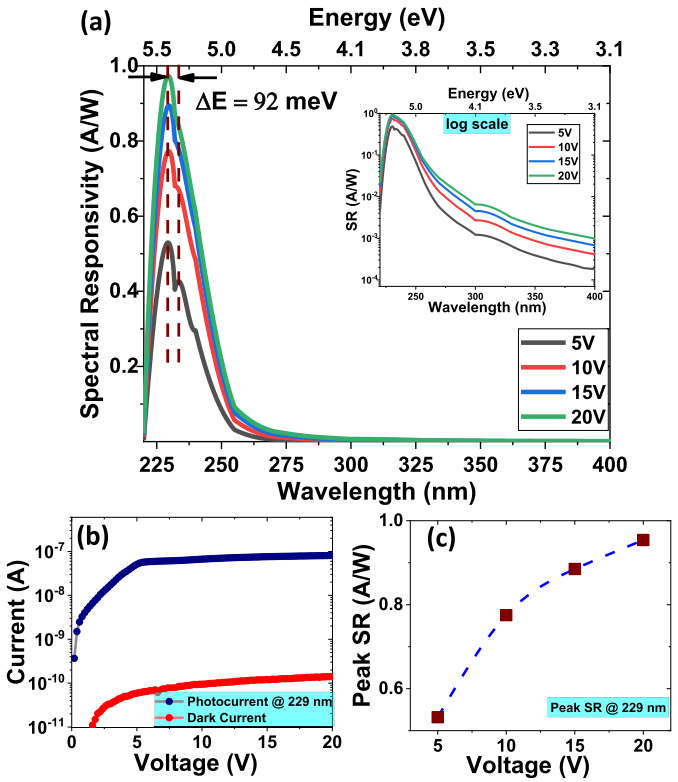

Fig. 5. (a). Spectral response as a function of voltage in linear scale, inset shows log scale revealing a UV-Visible rejection ratio $> 10^2$. (b) Photocurrent (at 229 nm) and dark current versus applied voltage. (c) Peak SR (at 229 nm) versus applied voltage.

where $a_{exc}$is effective the Bohr radius of the exciton, a_o is the Bohr radius of a hydrogen atom, ϵ_s is the static dielectric constant of α-Ga_2O_3, having value of 10 [4] and R_y is the Rydberg energy. a_{exc} of 8 Å corresponds to a dissociation field of 1.12 MV/cm.

Figure5 (a) shows the variation of responsivity with wavelength at different voltages on linear scale (5 V, 10 V, 15 and 20 V), the inset to figure 5(a) shows the same in log scale. The peak responsivity was measured to be 0.97 A/W at 229 nm at a bias of 20 V. The UV-to-visible rejection ratio was calculated by dividing the responsivity value at 229 nm by that at 400 nm and was found to be $>10^2$ at 20 V. The shoulder like feature at 233 nm (5.3 eV) in Fig 5(a) has been assigned to the excitonic transition. Similar feature was observed in the absorption spectra shown in Fig 3. This peak becomes less prominent at higher electric fields as expected. The other feature seen at 239 nm (5.18 eV) could be a phonon replica and it vanishes as the excitonic transition becomes weaker.

Figure 5(b) shows the current-voltage (I-V) characteristic of the detector under dark and under illumination at 229 nm. The photo current was found to be 85 nA while the dark current was measured to be 137 pA at an applied bias of 20 V, indicating a photo-to-dark current ratio exceeding two orders of magnitude.

Figure 5(c) shows the variation of peak responsivity with applied voltage under illumination at 229 nm. The peak responsivity was found to increase with an increase in applied voltage.

The theoretical value of responsivity at 229 nm, assuming a quantum efficiency of 100%, is 185 mA/W. This is much smaller than the peak responsivity value of 520 mA/W at 5 V (at 229 nm) measured in this work, even at a relatively low bias of 5 V, implying that there is gain in the devices [22]–[26]. This gain could be caused by oxygen vacancies [25], which act as hole trapping centres in the bulk of the semiconductor which could leads to photoinduced barrier lowering [22] resulting in an increase in transit time.

IV. Conclusion

In conclusion, we have reported on the study of growth and photo-response properties of mist CVD grown α-Ga_2O_3 on c-plane sapphire. Solar blind deep-UV photodetectors realized on these samples exhibited high responsivity of 0.5 A/W at 5 V bias with a sharp peak at 5.4 eV, low dark current of $\sim$ pA and UV-to-visible rejection ratio exceeding two orders of magnitude. We reported the first observation of excitonic peak in spectral responsivity with an excitonic binding energy of 90 meV. This work is expected to aid further in the understanding of optical properties of α-Ga_2O_3 towards realizing high-performance deep-UV optoelectronics based on gallium oxide.

Acknowledgment

The authors would like to acknowledge Micro Nano Characterization Facility (MNCF) and National Nano Fabrication Centre (NNFC) staff at CeNSE, IISc. They also like to thank Mr. Sooraj Sanjay and Mr. Mrityunjay Pandey.

References

[1] Y. Chen, X. Xia, H. Liang, Q. Abbas, Y. Liu, and G. Du, "Growth pressure controlled nucleation epitaxy of pure phase ϵ- and β-Ga_2O_3 films on Al_2O_3 via metal-organic chemical vapor deposition," *Cryst. Growth Des.*, vol. 18, no. 2, pp. 1147–1154, Jan. 2018.

[2] T. Wang, W. Li, C. Ni, and A. Janotti, "Band gap and band offset of Ga_2O_3 and $(Al_xGa_{1-x})_2O_3$ alloys," *Phys. Rev. A, Gen. Phys.*, vol. 10, no. 1, pp. 1–7, Jul. 2018.

[3] J. Furthmüller and F. Bechstedt, "Quasiparticle bands and spectra ofGa2O3polymorphs," *Phys. Rev. B, Condens. Matter*, vol. 93, no. 11, pp. 1–16, Mar. 2016.

[4] H. Masataka *et al.*, "Recent progress in Ga_2O_3 power devices," *Semicond. Sci. Technol.*, vol. 31, no. 3, p. 34001, 2016.

[5] A. S. Pratiyush *et al.*, "High responsivity in molecular beam epitaxy grown β-Ga_2O_3 metal semiconductor metal solar blind deep-UV photodetector," *Appl. Phys. Lett.*, vol. 110, no. 22, May 2017, Art. no. 221107.

[6] A. Trinchi, W. Wlodarski, and Y. X. Li, "Hydrogen sensitive Ga_2O_3 Schottky diode sensor based on SiC," *Sens. Actuators B, Chem.*, vol. 100, nos. 1–2, pp. 94–98, Jun. 2004.
[7] A. You, M. A. Y. Be, and I. In, "Deep-ultraviolet transparent conductive β-Ga_2O_3 thin films," *Appl. Phys. Lett.*, vol. 77, no. 25, p. 4166, 2017.
[8] L. Sang, M. Liao, and M. Sumiya, "A comprehensive review of semiconductor ultraviolet photodetectors: From thin film to one-dimensional nanostructures," *Sensors*, vol. 13, no. 8, pp. 10482–10518, Aug. 2013.
[9] M. Razeghi, "Short-wavelength solar-blind detectors-status, prospects, and markets," *Proc. IEEE*, vol. 90, no. 6, pp. 1006–1014, Jun. 2002.
[10] E. Monroy, F. Omnès, and F. Calle, "Wide-bandgap semiconductor ultraviolet photodetectors," *Semicond. Sci. Technol.*, vol. 18, no. 4, pp. R33–R51, Mar. 2003.
[11] A. Segura, L. Artús, R. Cuscó, R. Goldhahn, and M. Feneberg, "Band gap of corundumlike α-Ga_2O_3 determined by absorption and ellipsometry," *Phys. Rev. Mater.*, vol. 1, no. 2, Jul. 2017, Art. no. 024604.
[12] D. Shinohara and S. Fujita, "Heteroepitaxy of corundum-structured α-Ga_2O_3 thin films on α-Al_2O_3 substrates by ultrasonic mist chemical vapor deposition," *Jpn. J. Appl. Phys.*, vol. 47, no. 9, pp. 7311–7313, Sep. 2008.
[13] S. H. Lee *et al.*, "Sub-microsecond response time deep-ultraviolet photodetectors using α-Ga_2O_3 thin films grown via low-temperature atomic layer deposition," *J. Alloys Compounds*, vol. 780, pp. 400–407, Apr. 2019.
[14] X. H. Chen *et al.*, "Band alignment and band bending at α-Ga_2O_3/ZnO_{n-n} isotype hetero-interface," *Appl. Phys. Lett.*, vol. 115, no. 20, Nov. 2019, Art. no. 202101.
[15] G. T. Dang, T. Kawaharamura, M. Furuta, and M. W. Allen, "Mist-CVD grown Sn-doped α-Ga_2O_3 MESFETs," *IEEE Trans. Electron Devices*, vol. 62, no. 11, pp. 3640–3644, Sep. 2015.
[16] R. J. Elliott, "Intensity of optical absorption by excitons," *Phys. Rev.*, vol. 108, no. 6, pp. 1384–1389, Dec. 1957.
[17] Y. Toyozawa, "Theory of line-shapes of the exciton absorption bands," *Progr. Theor. Phys.*, vol. 20, no. 1, pp. 53–81, Jul. 1958.
[18] R. S. Knox, *Theory of Excitons*. New York, NY, USA: Academic, 1963.
[19] P. Jaiswal *et al.*, "Microwave irradiation-assisted deposition of Ga_2O_3 on III-nitrides for deep-UV opto-electronics," *Appl. Phys. Lett.*, vol. 112, no. 2, Jan. 2018, Art. no. 021105.
[20] M. C. Peter and Y. Yu, *Fundamentals of Semiconductors Physics and Materials Properties*, 4th ed. Cham, Switzerland: Springer, 2010.
[21] F. Schweiner, "Theory of excitons in cuprous oxide," Ph.D dissertation, Inst. Theor. Phys. I, Univ. Stuttgart, Stuttgart, Germany, Dec. 2017, doi: 10.18419/opus-9483.
[22] O. Katz, V. Garber, B. Meyler, G. Bahir, and J. Salzman, "Gain mechanism in GaN Schottky ultraviolet detectors," *Appl. Phys. Lett.*, vol. 79, no. 10, pp. 1417–1419, Sep. 2001.
[23] H. Srour *et al.*, "Solar blind metal-semiconductor-metal ultraviolet photodetectors using quasi-alloy of BGaN/GaN superlattices," *Appl. Phys. Lett.*, vol. 99, no. 22, Nov. 2011, Art. no. 221101.
[24] F. Xie *et al.*, "Metal–semiconductor–metal ultraviolet avalanche photodiodes fabricated on bulk GaN substrate," *IEEE Electron Device Lett.*, vol. 32, no. 9, pp. 1260–1262, Sep. 2011.
[25] A. M. Armstrong, M. H. Crawford, A. Jayawardena, A. Ahyi, and S. Dhar, "Role of self-trapped holes in the photoconductive gain of β-gallium oxide Schottky diodes," *J. Appl. Phys.*, vol. 119, no. 10, Mar. 2016, Art. no. 103102.
[26] S. Rathkanthiwar *et al.*, "Gain mechanism and carrier transport in high responsivity AlGaN-based solar blind metal semiconductor metal photodetectors," *J. Appl. Phys.*, vol. 121, no. 16, Apr. 2017, Art. no. 164502.